

Synchro-Curvature Self-Compton Radiation of Electrons in Curved Magnetic Fields

Bo Zhang^{1,2*}, Zi-Gao Dai^{1,2†}

¹*Department of Astronomy, Nanjing University, Nanjing 210093, P. R. China*

²*Key laboratory of Modern Astronomy and Astrophysics (Nanjing University), Ministry of Education, Nanjing 210093, P. R. China*

Accepted 00 00 00. Received 00 00 00; in original form 00 00 00

ABSTRACT

In this paper we present the spectrum of synchro-curvature self-Compton (SCSC) radiation of relativistic electrons with a power-law distribution of Lorentz factors. We find that the resulting spectrum is significantly different from that of either synchrotron self-Compton or curvature self-Compton radiation if both the curvature radius of the magnetic field and the cyclotron radius of the electrons are within some proper ranges. The effects of electrons' cooling and drifting, the low-energy self absorption in seed spectra, and the Klein-Nishina cutoff are also discussed, in order to get an accurate picture. We take gamma-ray bursts (GRBs) as our example environment for discussions. The results would be considered as a universal approach of the self-Compton emission of relativistic electrons moving in curved magnetic fields, and thus could be applied to many astrophysical phenomena, including GRBs, active galactic nuclei (AGNs), and pulsars.

Key words: radiation mechanisms: nonthermal - radiation mechanisms: general - relativity < Physical Data and Processes

1 INTRODUCTION

Traditionally, non-thermal radiation mechanisms of electrons in astrophysical environments are Bremsstrahlung, synchrotron radiation, curvature radiation, and inverse Compton scattering (e.g. see Blumenthal & Gould 1970, and Rybicki & Lightman 1979). Bremsstrahlung radiation is the result of collisions between charged particles, and has a continuous spectrum. Synchrotron emission arises from relativistic electrons moving around straight magnetic field lines, while curvature emission is radiated by electrons moving along curved field lines, and can be used to discuss the radiation from pulsar magnetosphere and AGNs (e.g., Cocke & Pacholczyk 1975). The formulae for calculating the characteristic frequencies and spectral energy distributions of these two radiation mechanisms are similar, while in the equations for curvature radiation the curvature radius replaces the cyclotron radius in the synchrotron radiation. In the high energy regime, the inverse-Compton scattering usually plays an important role. This type of emission occurs when relativistic electrons scatter low energy photons.

For electrons with a power law distribution of Lorentz factors, which are easily produced in astrophysical situations (e.g. products of shock acceleration, see Fermi 1949

and Grupe et al. 2005), the spectra of the resulting synchrotron and curvature radiations are also in the form of power laws. The difference is that, due to different relationships between Lorentz factor and critical frequency, their spectral power law indices for the same index p of electrons are not the same. The self-Compton emissions of these two radiation mechanisms have spectral shapes similar to that of seeds. Thus power law spectra, which are quite common under astrophysical conditions, are explained. If seed photons are from synchrotron radiation, which is the so-called synchrotron self-Compton radiation, a similar spectrum to the synchrotron seed is expected in this situation.

The synchro-curvature radiation depicting the spectrum emitted by electrons moving around curved magnetic field lines was first proposed by Zhang & Cheng (1995, 1996); Cheng & Zhang (1996), with a full set of formulae depicting the radiation spectrum, radiation power, characteristic frequency as well as polarization degree derived. The purpose of considering this radiation mechanism is to give some insights into new results which could not be interpreted well with conventional mechanisms only. The related quantum radiation equations for a single electron were given by Zhang & Yuan (1998), and the spectra from electrons with a power law energy distribution was calculated by Zhang et al. (2000). Harko & Cheng (2002) gave further discussions on electrons with larger transverse drifting velocities. As pointed out by Lieu & Axford (1997), the synchro-

* zhangbo@nju.edu.cn

† dzg@nju.edu.cn

curvature radiation should be considered as a more realistic treatment to the radiations by electrons in the universe.

Naturally, synchrotron and curvature radiations are the two limits of synchro-curvature radiation: the curvature radius is infinite for synchrotron radiation, while the electrons's cyclotron radius is zero for curvature radiation. The synchro-curvature radiation can be treated as a unified mechanism arising from relativistic electrons, and thus can be applied to general researches related to astrophysical radiations. It has already been used by to interpret radiation theories of pulsars by Zhang & Cheng (1997, 1998); Cheng & Zhang (1998); Hirotani et al. (2003), the energy excess of active galactic nuclei by Xia & Zhang (2001), as well as spectral observations of high energy photons from gamma-ray bursts observed in the Compton Gamma-Ray Observatory (CGRO) Era by Deng et al. (2005). As noted in Zhang et al. (2000), due to the non-power law items in the formulae describing the synchro-curvature radiation power, the spectrum is significantly deviated from all of the "traditional" mechanisms. Besides, the polarization degrees of synchro-curvature, synchrotron and curvature radiations are quite different from each other. So, from observed spectral shapes and the polarization measurements, one should distinguish between these three radiation mechanisms.

However, the synchro-curvature radiation alone cannot lead to a complete picture. As noted in Zhang et al. (2000), some other effects, such as the Compton scattering of this radiation mechanism, needs to be studied. Up to now synchro-curvature related inverse-Compton scattering has remained undiscussed. In this paper we calculate the spectrum of synchro-curvature self-Compton (SCSC) radiation, which makes the scheme of synchro-curvature radiation more complete, and present a more realistic approach to cosmic electron scattering. To our knowledge, this is the first work on the SCSC radiation mechanism. The structure of this paper is organized as follows. In section 2 basic equations of both synchro-curvature radiation and its self-Compton scattering are presented. In section 3 we show our numerical calculation results with various parameters, along with considerations of electron cooling, drifting and high energy Klein-Nishina cutoff. We carry out these calculations mainly for the case of gamma ray bursts, since these violent explosions are representatives of high energy astrophysical events, and can provide an extreme environment to discuss the high energy radiations. Our results are summarized in section 4.

2 BASIC EQUATIONS

In the following we consider the spectrum produced by relativistic electrons moving in curved magnetic fields. The circular magnetic field lines with constant curvature radius are assumed for simplicity in all of our calculations. Of course this is just a simplified treatment. In real situations, the curvature radius of a magnetic field line may vary from place to place, and thus the spectra will change accordingly. However, the basic equations for calculation remain the same. All we need to do then is to replace the curvature radius of field line with instant value.

First we present equations ignoring the electrons' drifts. As given in Zhang & Cheng (1995, 1996); Cheng & Zhang

(1996) and Zhang et al. (2000), the formula for the power per frequency of a single electron moving around a magnetic field line with curvature radius ρ is written as

$$\begin{aligned} \frac{dP}{d\omega} &= \frac{dP_{\perp}}{d\omega} + \frac{dP_{\parallel}}{d\omega} \\ &= \frac{\sqrt{3}e^2\gamma\omega}{4\pi r_c^*\omega_c} \left\{ \left[\int_{\omega/\omega_c}^{\infty} K_{5/3}(y) dy - K_{2/3}\left(\frac{\omega}{\omega_c}\right) \right] \right. \\ &\quad \left. + \frac{[(r_B + \rho)\Omega_0^2 + r_B\omega_B^2]^2}{c^4 Q_2^2} \left[\int_{\omega/\omega_c}^{\infty} K_{5/3}(y) dy \right. \right. \\ &\quad \left. \left. + K_{2/3}\left(\frac{\omega}{\omega_c}\right) \right] \right\}, \end{aligned} \quad (1)$$

and

$$\begin{aligned} \Omega_0 &= \frac{c \cos \alpha}{\rho}, \\ r_B &= \frac{c \sin \alpha}{\omega_B}, \\ \omega_B &= \frac{eB}{\gamma m_e c}, \\ r_c^* &= \frac{c^2}{(r_B + \rho)\Omega_0^2 + r_B\omega_B^2}, \\ \omega_c &= \frac{3}{2}\gamma^3 c \frac{1}{\rho} \left[\frac{(r_B^3 + \rho r_B^2 - 3r_B\rho^2)}{\rho r_B^2} \cos^4 \alpha + \frac{3\rho}{r_B} \cos^2 \alpha \right. \\ &\quad \left. + \frac{\rho^2}{r_B^2} \sin^4 \alpha \right]^{1/2}, \\ Q_2^2 &= \left(\frac{r_B^2 + \rho r_B - 3\rho^2}{\rho^3} \cos^3 \alpha \cos \theta_0 + \frac{3}{\rho} \cos \alpha \cos \theta_0 \right. \\ &\quad \left. + \frac{1}{r_B} \sin^3 \alpha \sin \theta_0 \right) \frac{1}{r_B}, \end{aligned}$$

where Ω_0 is the angular velocity of the moving electron's guiding center, r_B the cyclotron radius of the electron, ω_B the cyclotron frequency, r_c^* the instantaneous curvature radius of the electron's trajectory, ω_c the characteristic frequency of synchro-curvature radiation, and α the angle between field lines and the electron's injecting direction. Thus for power-law distributed relativistic electrons with distribution index p , the emissivity J_{ν} could be calculated according to following equations based on Zhang et al. (2000); Deng et al. (2005)

$$J_{\nu} = J_{\perp}(\nu) + J_{\parallel}(\nu), \quad (2)$$

and

$$\begin{aligned} J_{\perp}(\nu) &= \frac{\sqrt{3}e^2}{8\pi^2} \frac{9c^2}{4} \int N_0 \gamma^{-p+7} \frac{1}{\nu_c^2} \left\{ \frac{\nu}{\nu_c} \left[\int_{\nu/\nu_c}^{\infty} K_{5/3}(y) dy \right. \right. \\ &\quad \left. \left. + K_{2/3}\left(\frac{\nu}{\nu_c}\right) \right] \right\} \times \left(a_0 \gamma + a_1 + \frac{a_2}{\gamma} \right)^3 d\gamma, \\ J_{\parallel}(\nu) &= \frac{\sqrt{3}e^2}{2} \int N_0 \gamma^{-p+1} \left\{ \frac{\nu}{\nu_c} \left[\int_{\nu/\nu_c}^{\infty} K_{5/3}(y) dy \right. \right. \\ &\quad \left. \left. - K_{2/3}\left(\frac{\nu}{\nu_c}\right) \right] \right\} \times \left(a_0 \gamma + a_1 + \frac{a_2}{\gamma} \right) d\gamma, \end{aligned}$$

where we replace the circular frequency ω with angular frequency $\nu = \omega/2\pi$ for convenience. The above two equations give the emissivity in two polarizations, with $a_0 =$

$\frac{m_e c^2 \sin^2 \alpha \cos^2 \alpha}{e B \rho^2}$, $a_1 = \frac{\cos^2 \alpha}{\rho}$, and $a_2 = \frac{e B \sin \alpha}{m_e c^2}$. Therefore it is clearly seen that $a_0 \gamma + a_1 + \frac{a_2}{\gamma} = \frac{1}{r_c^*}$.

While in real situations, electrons may not stay around one magnetic field line; on the contrary, they can drift due to inhomogeneous curved magnetic fields. This idea that charged particles can have different motion in inhomogeneous magnetic field has already been proposed several decades ago (e.g., see Chugunov et al. 1975), while the unified formulae for single relativistic electron's synchro-curvature radiation spectrum with electrons' transverse drift velocity considered was given by Harko & Cheng (2002) as follows:

$$\frac{dP}{d\nu} = \frac{\sqrt{3}e^3}{m_e c^2} \left[B^2 \sin^2 \alpha + 2 \frac{\gamma m_e B}{e} \frac{v_{\parallel}^2 + \frac{1}{2} v_{\perp}^2}{\rho} \sin \alpha + \frac{\gamma^2 m_e^2 (v_{\parallel}^2 + \frac{1}{2} v_{\perp}^2)^2}{e^2 \rho^2} \right]^{1/2} F\left(\frac{\nu}{\nu_c}\right), \quad (3)$$

where the characteristic frequency ν_c is defined by

$$\nu_c = \frac{3e}{2m_e c} \left[B^2 \sin^2 \alpha + 2 \frac{\gamma m_e B}{e} \frac{v_{\parallel}^2 + \frac{1}{2} v_{\perp}^2}{\rho} \sin \alpha + \frac{\gamma^2 m_e^2 (v_{\parallel}^2 + \frac{1}{2} v_{\perp}^2)^2}{e^2 \rho^2} \right]^{1/2} \frac{\gamma^2}{2\pi}, \quad (4)$$

where $F(x) = x \int_x^\infty K_{5/3}(y) dy$, α the angle between field lines and the electron's injecting direction, $v_{\parallel} = v \cos \alpha$ the electron's velocity component parallel to the field, $v_{\perp} = v \sin \alpha$ the electron's velocity perpendicular to the field, and the electron's velocity v can be calculated from the Lorentz factor γ . It can be clearly seen that due to electrons' drift, the spectral shape and flux are changed significantly. Similar to the calculations for non-drifting electrons, the emissivity of power law distributed electrons can be easily derived from Eq.(3), with electrons' distribution function multiplied with single electron's spectrum.

In Figure 1 we present the ratio between radiation powers at characteristic frequency of synchro-curvature radiation without and with the consideration of electrons' transverse drift velocity with the various B and ρ used below. We fix the Lorentz factor as $\gamma = 3 \times 10^3$, which is typical for gamma ray bursts. It can be seen that the relation between the ratio and the magnetic field, especially between the ratio and B is quite complex.

Similar to other traditional radiation mechanisms, the synchro-curvature radiation may show self absorption features in the low energy part in some situations. As noted in Yang et al. (2003), the absorption coefficients of the two polarization components in vacuum are

$$K_{\nu, \perp} = \frac{p+2}{4\pi m_e \nu^2} \frac{\sqrt{3}e^2}{2} \int N_0 \gamma^{-(p+1)} \frac{\gamma}{Q_2^2 r_c^*} \times \left[\int_{\nu/\nu_c}^\infty K_{5/3}(y) dy + K_{2/3} \right] d\gamma, \quad (5)$$

$$K_{\nu, \parallel} = \frac{p+2}{4\pi m_e \nu^2} \frac{\sqrt{3}e^2}{2} \int N_0 \gamma^{-(p+1)} \frac{\gamma}{r_c^*}$$

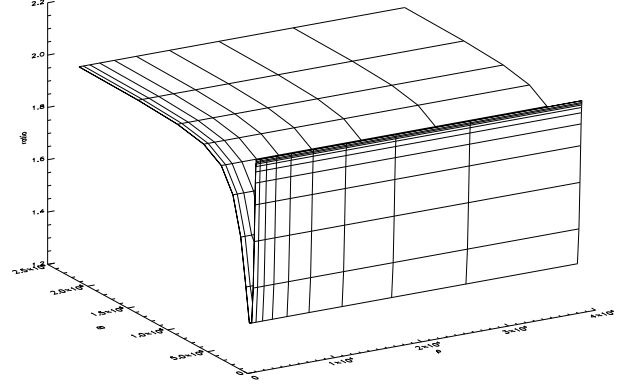


Figure 1. The ratio of synchro-curvature radiation's radiation powers at characteristic frequency without and with the consideration of electrons' transverse drift velocity in magnetic fields with various parameters. X-axis denotes different values of curvature radius ρ , while y-axis denotes different B .

$$\times \left[\int_{\nu/\nu_c}^\infty K_{5/3}(y) dy - K_{2/3} \right] d\gamma.$$

While in plasma environment, the coefficients may have some changes. We take Eq.(2) and Eq.(3) as low energy seed spectra to calculate the self-Compton spectrum of synchro-curvature radiation, and consider the possible effects of self absorption. The IC emissivity can be expressed as (e.g. Sari & Esin 2001)

$$j_\nu^{IC} = 3\sigma_T \int_{\gamma_m}^{\gamma_{max}} d\gamma N(\gamma) \int_0^1 dx f_{\nu_s}^\dagger(x) g(x) \quad (6)$$

with $x = \frac{\nu}{4\gamma^2 \nu_s}$ and $g(x) = 1 + x + 2x \ln x - 2x^2$. Here $f_{\nu_s}^\dagger$ means the incident specific flux of frequency ν_s at the scattering region, and can be related with the original seed flux f_{ν_s} by the formula $f_{\nu_s} = f_{\nu_s}^\dagger \frac{4\pi R^2}{4\pi D^2}$, with R being the radius of the scattering region and D being the distance to the observer. And ν is the frequency of IC scattering, while ν_s is the frequency of the incident seed emission.

The formulae above are only suitable in the Thomson limit. For the high energy Klein-Nishina regime, we adopt the equation proposed by Jones (1968) and quoted by Blumenthal & Gould (1970) with modified scattering cross section,

$$j_\nu^{IC} = 3\sigma_T \int_{\gamma_m}^{\gamma_{max}} d\gamma N(\gamma) \int_{\nu_{s,min}}^{\nu_s} d\nu_s \frac{\nu f_{\nu_s}^\dagger}{4\gamma^2 \nu_s^2} [2y \ln y + y + 1 - 2y^2 + \frac{1}{2} \frac{x^2 y^2}{1+xy} (1-y)], \quad (7)$$

where h denotes the Plank constant, $x = 4\gamma h \nu_s / (m_e c^2)$, $y = h\nu / [x(\gamma m_e c^2 - h\nu)]$, $\nu_{s,min} = \nu m_e c^2 / [4\gamma(\gamma m_e c^2 - h\nu)]$, and $\gamma > h\nu / (m_e c^2)$.

Considering the polynomial items in the equations of the seed spectrum, especially the ones that are $a_0 \gamma + a_1 + a_2/\gamma$ for non-drifting electrons and $\sqrt{B^2 \sin^2 \alpha + 2 \frac{\gamma m_e B}{e} \frac{v_{\parallel}^2 + \frac{1}{2} v_{\perp}^2}{\rho} \sin \alpha + \frac{\gamma^2 m_e^2 (v_{\parallel}^2 + \frac{1}{2} v_{\perp}^2)^2}{e^2 \rho^2}}$ for drifting electrons, we need to calculate the integrations above. The characteristic frequency of SCSC is no longer

a simple power law function of the electron Lorentz factor. On the contrary, since different item dominates in different band, the relationship between characteristic frequency and Lorentz factor can be quite complex. Zhang et al. (2000) have already shown that the seed synchro-curvature radiation spectra arising from a power-law distributed electrons are quite different from simple power law. Thus, a similar deviation is expected for SCSC.

3 NUMERICAL RESULTS

In the calculations below, we suppose that all of the electrons are distributed isotropically for simplicity. In order to calculate the modified Bessel functions of fractional order in the equations in Section 2, we adopt the code provided by Chapter 6 of Press et al. (1992).

In the calculations we mainly consider the situation of gamma-ray bursts. GRBs are the strongest explosions in the universe since the Big Bang, and the existence of strong magnetic fields as well as relativistic electrons are implied both observationally and theoretically (e.g., see Piran 1999). For this reason, such events are often considered as laboratory to test some high energy process in astrophysics. Deng et al. (2005) applied the synchro-curvature radiation to interpret the high energy excess observed by CGRO, and got reasonable fitting results compared with other works using traditional radiation mechanisms (e.g., see Tavani 1996). The advantage of their work is that, by introducing the synchro-curvature radiation, the number of free parameters can be reduced, thus a more convenient treatment can be achieved. Here we adopt the parameters similar to the fittings listed in Deng et al. (2005). As noted in Piran (1999) and Guetta & Granot (2003), typically speaking, the bulk Lorentz factor of GRBs is $\Gamma \sim 10^2 - 10^3$, magnetic field $B \sim 10^4$, and electrons' minimum Lorentz factor $\gamma_{min} \sim 10^2 - 10^3$. The fitting results provided by Deng et al. (2005) are around $\Gamma [\gamma_{min}^2 B]_{12} \sim 10$ and $\Gamma [\gamma_{min}^3 / \rho]_8 \sim 10$, where $[\gamma_{min}^2 B]_{12} = \gamma_{min}^2 B / 10^{12}$ and $[\gamma_{min}^3 / \rho]_8 = (\gamma_{min}^3 / \rho) / 10^8$.

These results yield relatively small curvature radius of magnetic field. In theory, several magnetic field configuration models have been proposed for GRBs. As noted in Rossi et al. (2004), one of the most popular models is that, the magnetic field in the GRB jets can be produced by the shock, and are compressed into a thin layer normal to the propagation direction. Since the field in such a layer is highly tangled, small scale variations of magnetic field (therefore small value for field's characteristic curvature radius ρ) can be achieved. Some numerical simulations on GRB magnetic field involving the two stream (Weibel) instability also give rise to similar long-lasting field structure, especially in internal shocks. (e.g. see Medvedev & Loeb 1999, Medvedev et al. 2005 and references herein). And according to Medvedev (2000) and Mizuno et al. (2010), small scale structures of fields can dominate in the case of GRBs. In such situations, it is possible that synchro-curvature radiation as well as SCSC can play an important role in shaping the GRBs' spectrum.

First we show the seed spectra samples in Figure 2. The solid line, dotted line and dashed line correspond to the spectrum of synchro-curvature radiation, synchrotron radiation, and curvature radiation respectively.

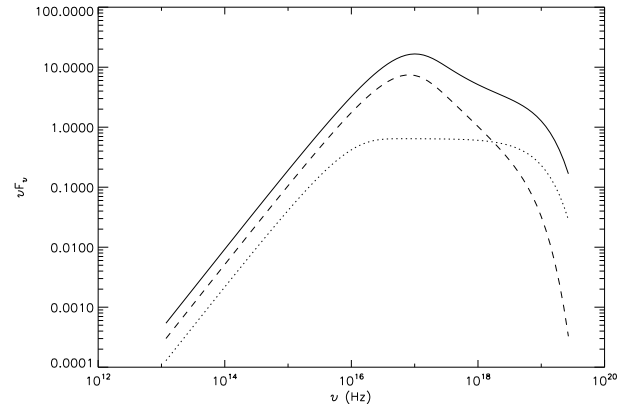


Figure 2. Spectra of synchro-curvature radiation (solid line), synchrotron radiation (dashed line), and curvature radiation (dotted line) with magnetic field $B = 10^4$ Gauss, curvature radius of field $\rho = 10^3$ cm, minimum electron Lorentz factor $\gamma_{min} = 10^3$, maximum Lorentz factor $\gamma_{max} = 10^4$, and electron distribution index $p = 5$. Fluxes are in arbitrary unit.

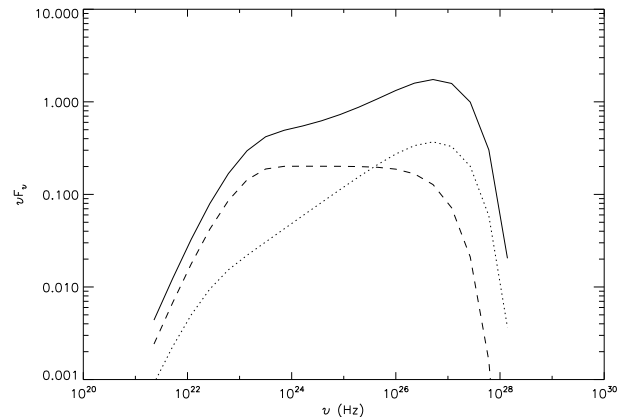


Figure 3. Self Compton spectra of synchro-curvature radiation (solid line), synchrotron radiation (dashed line), and curvature radiation (dotted line). Parameters are the same as in Figure 1.

From Figure 2, we can see that for synchrotron radiation rising from electrons with power law distribution of Lorentz factors, the spectral index should be $(p - 1) / 2$ (where p is the power law index of electrons). While for curvature radiation, the index is $(p - 2) / 3$. However, due to polynomial items in the synchro-curvature radiation formulae, the resulting spectrum cannot be described with a single power law. Thus a turnoff is expected for self-Compton emission, and corresponding to a point where a different item in the polynome dominates. Roughly speaking, this is the point when $a_0 \gamma = a_2 / \gamma$. Figure 3 shows the corresponding IC spectrum of Figure 2.

Figures 2 and 3 show the spectra of electrons with a large power law index ($p = 5$). For shock acceleration which is common in astrophysical circumstances, electrons usually have a smaller index, $p \sim 2 - 2.5$. We present calculational results for such electrons in Figure 4.

It is noted that for a smaller index p , the spectrum doesn't show a significant turnoff. We try to find some explanations for this phenomena. In the seed spectrum, synchrotron and curvature radiations have different spectral in-

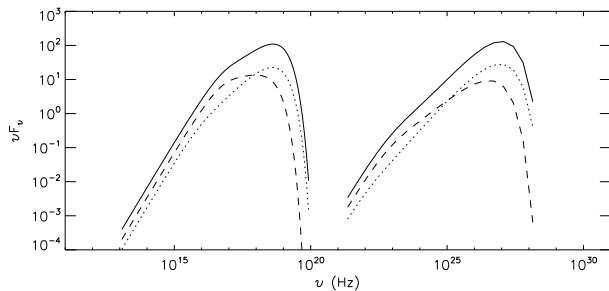


Figure 4. Synchro-curvature radiation (solid line), synchrotron radiation (dashed line), and curvature radiation (dotted line) spectra (left) and corresponding self Compton spectra (right) for electron collective with $p = 2.5$. Other parameters are the same as in Figure 1.

dex α . Although the synchro-curvature emission is not a simple addition to the former two traditional radiation spectra, we can see that the synchro-curvature spectrum can be considered as a summation of synchrotron and curvature plus the coupling items. If electrons can have cyclotron radius value similar to magnetic field's curvature radius (which mean the contributions from synchrotron and curvature radiations are comparable with each other), as well as large difference between spectral indices for synchrotron and curvature radiations, the high energy turnoff can be very evident. For parameters within the ranges used in our calculation, it is seen from Figures 2, 3 and 4 that for a smaller curvature radius, weaker magnetic fields and larger electron index p , synchrotron and curvature radiations overlay more significantly. Since the resulting self Compton emissions have similar (although smoother) spectral shapes to seeds, turnoff points are expected naturally.

The turnoffs can also be explained by the equations describing the resulting spectrum. The ratio of the $a_0\gamma$ to a_2/γ items of the polynomy ($a_0\gamma + a_1 + a_2/\gamma$) can change a lot across the observed energies. So the spectral index may change from one frequency range to another. Comparing their relative values, we can get an overall idea of the position of the turnoff point. Figure 2 from Zhang et al. (2000) gives an example of the relationship between the magnetic field B and the energy of turnoff point. For self-Compton scattering a similar relationship is expected.

Besides, if we change γ_{max} to a larger value, the shape of the high energy turnoff can also be affected. Usually the larger γ_{max} , the longer the excess part. The exact value of γ_{max} is related to the particle acceleration and radiation mechanisms, e.g., in the case of gamma ray bursts, electrons whose shock acceleration timescale equals to cooling timescale of non-thermal radiation have the maximum Lorentz factor (e.g. see Dai & Lu 1998). Thus the value γ_{max} can be calculated. And the values of B , ρ and so on also affect the final shape of the spectra: smaller B and ρ lead to a more significant spectral deviation from traditional IC scattering, while spectra formed in magnetic fields with larger B and larger curvature radius ρ are nearly identical with SSC radiation.

Similar to other types of inverse Compton scattering, the polarization of SCSC depends on the magnetic field structure, the distribution of emitting photons, as well as viewing angle. Anisotropic electrons can give rise to signif-

icant polarized IC emission (e.g. see Begelman & Sikora 1987). As noted by Beloborodov et al. (2010), usually in previous works related to GRBs, isotropic electrons are assumed (e.g., see Granot et al. 1999), although this may not be the real situation. With random fields, the seed spectra from the whole jet do not have large degrees of polarization; the polarized signals from different regions are wiped out. Thus one can not expect too much degrees of polarization for SCSC emission in the comoving frame. Since the polarization degree remains the same with Lorentz transformation, the observed emission for on-axis observer does not show significant polarization either. However anisotropy emerges to the off-axis observers. Thus polarization patterns for SCSC exist in this situation, and are differs from traditional radiation mechanisms, especially in the high energy regime, since the polarization can be affected by the spectral shape. Besides, it is possible that non-zero polarization degree arise from the underlying field with some degree of order, that is, the field is not totally random. And some works also show that relativistic electrons do have some anisotropy in the comoving frame (e.g., see Achterberg et al. 2001). Some recent works on GRBs have taken anisotropy of electrons into account (e.g., see Beloborodov et al. 2010), although this issue need to be discussed in more details. Therefore more detailed simulations may be needed to describe the real polarization behavior.

Finally we consider the self absorption effects of the synchro-curvature seed spectrum. Since the absorption only show significant effects in the low energy regime, changing the spectra index, while the differences between SCSC and other traditional mechanisms are mainly in the high energy portion (that is, the high energy turnoff), the self absorption effects do not matter a lot in our discussion. So we do not consider this issue in the following calculations for simplicity. In fact, for synchro-curvature seed radiation in vacuum, the major absorption part is quite similar to synchrotron self absorption, with the spectrum proportional to $\nu^{5/2}$, and only a bit flatter in the higher energy part of the absorption regime, as noted in Yang et al. (2003). However, negative self absorption may occur in plasma environment, although still affect the low energy part only.

3.1 Cooling Effect of Electrons in the Case of Gamma-Ray Bursts

Integration over the electron Lorentz factor γ is needed to get the whole spectrum. In the calculation of the spectra shown in Figures 2 to 4, a simple power law distribution is assumed. However, under real astrophysical circumstances, the cooling effect of electrons should be considered in order to get an accurate spectrum, e.g., in the situation to calculate the spectrum of gamma-ray bursts (e.g., see Sari, Piran & Narayan 1998). Here we take this issue into account, and discuss the fast and slow cooling regimes for GRBs under the framework of SCSC.

Let p denote the initial power law index. For fast cooling electrons, all of the electrons can cool down to about the cooling Lorentz factor (at which the cooling timescale equals to the dynamical timescale of the system). In this situation, the distribution function should be

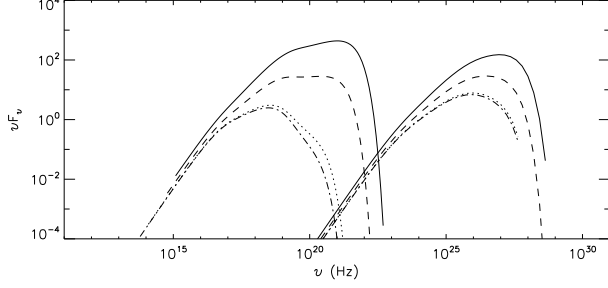


Figure 5. Curves on the left show the synchro-curvature radiation spectra of fast cooling electrons with index $p = 5$, magnetic field $B = 10^4$ Gauss and curvature radius $\rho = 0.5 \times 10^3$ cm (solid line), $\rho = 1 \times 10^3$ cm (dashed line), $\rho = 5 \times 10^3$ cm (dotted line), and $\rho = 10 \times 10^3$ cm (dashed dotted line). The corresponding self Compton spectra are shown on the right. All of the spectra are in arbitrary units.

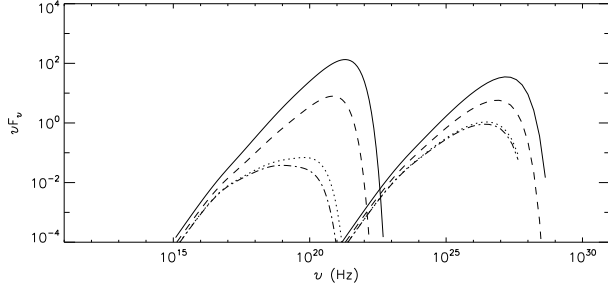


Figure 6. Curves on the left show the synchro-curvature radiation spectra of fast cooling electrons with index $p = 2.5$, magnetic field $B = 10^4$ Gauss and curvature radius $\rho = 0.5 \times 10^3$ cm (solid line), $\rho = 1 \times 10^3$ cm (dashed line), $\rho = 5 \times 10^3$ cm (dotted line), and $\rho = 10 \times 10^3$ cm (dashed dotted line). The corresponding self Compton spectra are shown on the right. All of the spectra are in arbitrary units.

$$N(\gamma) = \begin{cases} n_\gamma \gamma^{-2}, & \gamma_c < \gamma < \gamma_m \\ n_\gamma \gamma_m^{p-1} \gamma^{-p-1}, & \gamma_m < \gamma < \gamma_{max}, \end{cases} \quad (8)$$

where $n_\gamma = \gamma_c n_e$, n_e is the number of electrons, γ_m the minimal Lorentz factor, γ_c the cooling Lorentz factor, and γ_{max} the maximum Lorentz factor. In the fast cooling regime, $\gamma_c < \gamma_m < \gamma_{max}$. Under such conditions, the spectra of synchro-curvature emission and its self Compton radiation are drawn in Figures 5 and 6.

For slow cooling electrons, $\gamma_m < \gamma_c < \gamma_{max}$, and $n_\gamma = (p-1) \gamma_m^{p-1} n_e$. The electron distribution is

$$N(\gamma) = \begin{cases} n_\gamma \gamma^{-p}, & \gamma_m < \gamma < \gamma_c \\ n_\gamma \gamma_c \gamma^{-p-1}, & \gamma_c < \gamma < \gamma_{max}. \end{cases} \quad (9)$$

In Figures 7 and 8, sample spectra of slow cooling electrons are presented. It is clearly seen that the electron cooling effect makes the low energy index of electrons smaller, thus making the resulting spectrum nearly identical with synchrotron self-Compton radiation, especially for fast cooling electrons that have a smaller low energy index. For slow cooling electrons with a larger low energy index, the difference between SSC and SCSC becomes more significant.

For other astrophysical objects, e.g., the cooling effects can be different. Kardashev (1962) has given a detailed view of this issue.

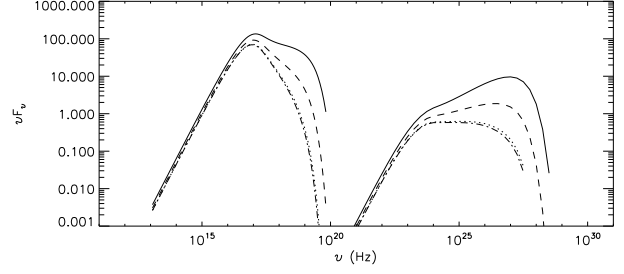


Figure 7. Curves on the left show the synchro-curvature radiation spectra of slow cooling electrons with index $p = 5$, magnetic field $B = 10^4$ Gauss and curvature radius $\rho = 0.5 \times 10^3$ cm (solid line), $\rho = 1 \times 10^3$ cm (dashed line), $\rho = 5 \times 10^3$ cm (dotted line), and $\rho = 10 \times 10^3$ cm (dashed dotted line) as IC scattering seeds. The corresponding self Compton spectra are on the right. All of the spectra are in arbitrary units.

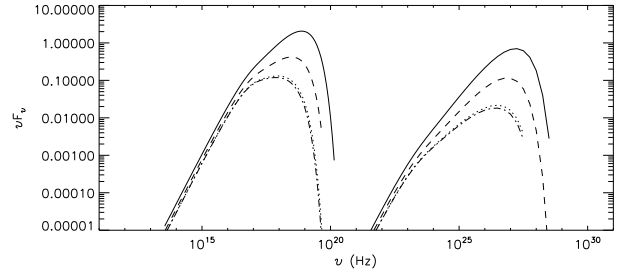


Figure 8. Curves on the left show the synchro-curvature radiation spectra of slow cooling electrons with index $p = 2.5$, magnetic field $B = 10^4$ Gauss and curvature radius $\rho = 0.5 \times 10^3$ cm (solid line), $\rho = 1 \times 10^3$ cm (dashed line), $\rho = 5 \times 10^3$ cm (dotted line), and $\rho = 10 \times 10^3$ cm (dashed dotted line) as IC scattering seeds. The corresponding self Compton spectra are shown on the right. All spectra are in arbitrary units.

3.2 Spectra of Drifting Electrons

As shown in Section 2, the resulting synchro-curvature radiation can be changed if electron drifts exist due to inhomogeneous magnetic field. The formulae describing drifting electrons' spectra are quite different from the ones emitted by non-drifting electrons. Thus the self Compton emission from such electrons is also not the same as simple SCSC shown above. Here we calculate drifting electrons' synchro-curvature self Compton radiation.

In Figure 9 we show the seed and self Compton spectra of synchro-curvature radiation with and without drifts, as well as the synchrotron and curvature radiations. Because of the difference in the distribution of seed photons, the drifting effects can change the resulting SCSC spectra significantly, especially in the high energy regime.

For non-drifting electrons, the high energy regime in the SCSC spectra is mainly contributed by the curvature self Compton radiation. The large transverse velocity can suppress the electrons' motion along magnetic field lines and thus suppress the curvature radiation part. Thus such deviation can be explained.

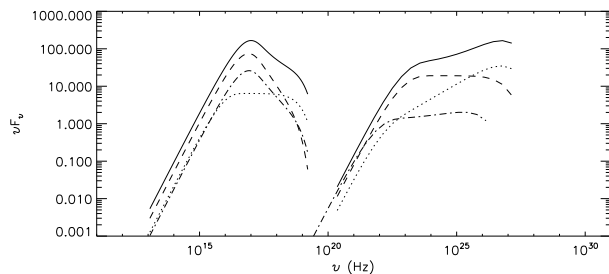


Figure 9. Spectra on the left are from the synchro-curvature radiation without drifts (solid line), the synchro-curvature radiation with drifts (dash-dotted line), the synchrotron radiation (dashed line), and the curvature radiation (dotted line) with $B = 0.5 \times 10^4$ Gauss, $p = 5$ and $\rho = 10^3$ cm. The corresponding self Compton spectra are shown on the right. All of the spectra are in arbitrary units.

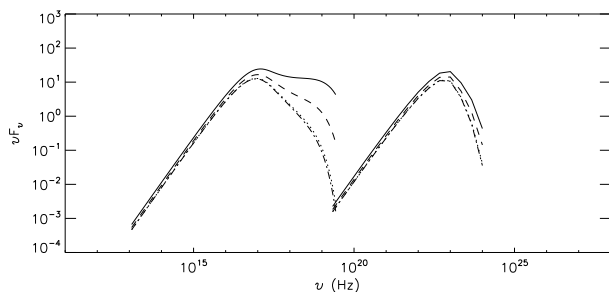


Figure 10. Spectra on the left are from the synchro-curvature radiation spectra of electrons with index $p = 5$ and curvature radius $\rho = 0.5 \times 10^3$ cm (solid line), $\rho = 1 \times 10^3$ cm (dashed line), $\rho = 5 \times 10^3$ cm (dotted line), and $\rho = 10 \times 10^3$ cm (dashed dotted line). The corresponding self Compton spectra with KN cross section correction are shown on the right. All of the spectra are in arbitrary units.

3.3 Klein-Nishina Corrected Spectrum

All of the spectra presented above are calculated in the Thomson limit. For high energy photons, i.e., $\gamma h\nu > m_e c^2$, where ν denotes the frequency, and γ the Lorentz factor of electrons, the scattering cross section does not remain constant as the Thomson cross section σ_T . In this situation, the Klein-Nishina cross section formula should be applied instead of σ_T . Some Klein-Nishina corrected synchro-curvature spectrum samples with various parameters are presented in Figures 10 and 11.

From Figures 10 and 11 it is clearly seen that due to the high energy suppression of the Klein-Nishina scattering cross section, the high energy turnoff of SCSC radiation in the Thomson limit no longer exists. So we conclude that the difference between SCSC and SSC could not be significant when the Klein-Nishina cutoff is dominated.

4 SUMMARY AND DISCUSSIONS

In this paper we present the spectrum of the SCSC radiation for various parameters and situations. We here summarize all of the results listed above:

First of all, the real radiation mechanism for relativistic electrons in magnetic fields could not be the synchrotron or

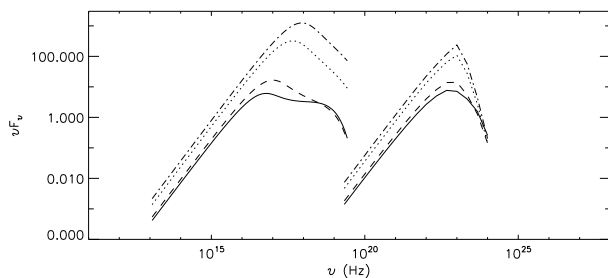


Figure 11. Spectra on the left are from the synchro-curvature radiation spectra with different magnetic fields. The solid line shows spectrum with $B = 0.5 \times 10^4$ Gauss, the dashed line $B = 1 \times 10^4$ Gauss, the dotted line $B = 5 \times 10^4$ Gauss, and the dashed dotted line $B = 10 \times 10^4$ Gauss. The corresponding KN corrected self Compton spectra (right) are for electron collective with $p = 5$. Other parameters are the same as in Figure 10.

curvature radiation. On the contrary, the synchro-curvature radiation provides a more realistic treatment. Thus a similar situation is expected for self Compton scattering. If the seed spectrum is synchro-curvature rather than other traditional mechanisms, the inverse-Compton spectrum could still be an open question. In fact, it can be seen from the contents above that the resulting spectra deviates from the form of simple power law, especially for electrons with a larger distribution index and the drifts of electrons in magnetic fields are ignored. A curved magnetic field can significantly changes the resulting spectrum. Thus SSC alone can not precisely describe the real IC spectra. Combined with the synchro-curvature seed, multiple turnoffs in the whole spectrum could be expected.

Second, the resulting inverse-Compton spectrum of synchro-curvature radiation can be affected by various parameters, including the strength of the magnetic field B , the curvature radius of the field ρ , the index of the electron energy distribution p , and so on. For example, a smaller curvature radius ρ and a smaller field strength B usually leads to a more significant high energy turn off. The resulting spectra from electrons with a smaller distribution index resembles to synchrotron self Compton radiation, while for electrons with a larger index of the Lorentz factor distribution, the self-Compton spectrum of synchro-curvature radiation clearly shows a high energy turnoff in the Thomson regime. Besides, drifting effects of electrons due to inhomogeneous magnetic field can also change the SCSC spectra, with different shapes of turnoffs. This phenomena can be attributed to the different relations between the characteristic frequency and the radius of electrons' motion for synchrotron and curvature radiations (the SCSC spectrum is something like the summation of the synchrotron and curvature self-Compton radiations, although not exactly), as well as the polynomial items in the formulae describing the spectrum. So the high energy self-Compton spectra of a certain astrophysical source may also used as a possible probe of seed radiation mechanisms, and the spatial and temporal variations of radiation spectra can reveal the changes in magnetic field.

Third, the cooling process of electrons can change the electron distribution index. As a result, the resulting scattering spectra is also changed. As noted above, the high energy turnoff of SCSC radiation only becomes significant

when the electron distribution index is large. Fast cooling electrons have a relatively small low energy index, and they could suffer more influences. So the high energy turnoff may be not as significant as expected in real situations.

Fourth, it should be noticed that the calculations in Section 3 are all based upon the assumption of isotropically distributed electrons. We calculated the electrons with δ -shape distribution function as well, and the resulting spectra are quite similar to the ones from isotropic electrons. However, the spectra might be slightly different from the sample results presented in this paper for electrons with other forms of spatial distribution.

Fifth, the self absorption (positive for vacuum, both positive and negative are possible for plasma) may occur in the synchro-curvature seed spectrum. However, this absorption is only evident in the low energy part, thus nearly have no effect on the high energy regime. Since the SCSC radiation differs from traditional radiation mechanisms mostly in the high energy band, self absorption is not a major concern for the calculated SCSC radiation spectra and distinguishing SCSC from other mechanisms.

Sixth, since we mainly discuss the self Compton radiation for isotropically distributed electrons from GRB shock acceleration, the polarization in the seed spectra can be nearly wiped out by random electrons. So the polarization degree is nearly zero in the scattering spectrum for on-axis observers. This may not be the real situation, and high polarization degree may exist for off-axis observations, highly anisotropic electrons, or magnetic fields with a certain preferred direction. While the exact value of the degree depends on the configuration of electrons' distribution, and careful simulations may be required to calculate this.

Finally, in the Klein-Nishina regime, the difference between SCSC and SSC radiation as well as other traditional forms of inverse-Compton scattering is relatively small due to strong high energy suppression. Although the difference could not be ignored in the Thomson regime, in the Klein-Nishina limit it seems difficult to distinguish between the synchro-curvature self Compton radiation from traditional inverse-Compton scattering.

The detection of synchro-curvature radiation as well as SCSC can provide vital clues of the structure of magnetic field. Here we also take GRB as example. The field configuration in the jet may be randomly distributed (as noted in Section 3) or ordered field (e.g., see Toma et al. 2009 and references herein). One way to distinguish these two models is to measure the polarization in the GRB emissions. However, current instruments are not quite suitable for this task; no reliable polarization measurement on high energy emission has been obtained yet. However, if one can analyze the spectrum and find out any synchro-curvature or SCSC component, this could lead to a conclusion that random field may be the real configuration; since ordered magnetic field have nearly straight field lines, and thus can not produce synchro-curvature radiation. On the other hand, if both of the spectral signature and polarization degree can be measured in the future, the understanding on GRB magnetic field will be greatly improved.

As noted at the beginning of Section 2, in this paper only circular field lines are considered. While in real astrophysical environments, the curvature radius of magnetic fields usually changes from place to place, as one can ex-

pected. Thus these calculations only show the emission from a certain area at a certain time, and analyzing the spectra's spacial behavior (for extended sources) and temporal evolution can provide some insights into the structure of the magnetic fields at the source region. For example, if one can detect the transition between synchro-curvature/SCSC radiation and other traditional radiation mechanisms in a single source, the magnetic field distribution can be unveiled, at least in some degrees.

Similar to the synchro-curvature seed spectrum, the self-Compton spectrum presented in this paper should be considered as the baseline of IC scattering calculations, and can be used universally to explain the high energy observations (especially the "abnormal" spectral behavior, including the high energy excess), and can be applied to nearly all high energy astronomical objects, e.g., active galactic nuclei, gamma-ray bursts, and pulsars. For example, as noted in Deng et al. (2005), several GRBs observed in the CGRO era have high energy turnoffs; and similar spectral features has also been detected by Fermi Gamma Ray Space Telescope, with possible high energy exponential cutoff observed in one burst (GRB 090926A, e.g., see Ackermann et al. 2010). The SCSC provides another possible explanation for these facts, since SCSC spectra yield high energy turnoff, while limited maximum Lorentz factor can naturally give rise to high energy cutoff. And KN effects of SCSC can provide sharp cutoff as well. Here multiband data is required in order to tell the real radiation mechanism beneath. And probing the real mechanism through high energy observations is also possible, especially for a large energy index of electrons, although in the Klein-Nishina regime things can be a bit more difficult.

Of course, the high energy turnoff in observational data could be easily explained by the superimposition of several spectra arising from different mechanisms, so it's a complicated task to confirm the contributions from synchro-curvature radiation and its self Compton scattering, especially when the scattering occurs in the Klein-Nishina limit with strong high energy suppression (thus the overall spectrum may not show multiple turnoffs). In order to solve this problem, temporal data are required. If both the low energy part and the high energy turnoff evolve simultaneously, SCSC radiation is a possible radiation mechanism; or several mechanisms will take the responsibility, since different mechanisms usually show different temporal behaviors. However exceptions may also exist in the latter case, since the structure change of a magnetic field can also lead to different spectra at different times.

ACKNOWLEDGMENTS

The authors thank Bing Zhang for helpful discussions and an anonymous referee for valuable comments that have allowed us to improve the manuscript. This work is supported by the National Natural Science Foundation of China (grant no. 10873009 and 11033002) and the National Basic Research Program of China (973 program) No. 2007CB815404.

REFERENCES

- Achterberg A., Gallant Y. A., Kirk, J. G., Guthmann A. W., 2001, MNRAS, 328, 393
- Ackermann M. et al. 2010, ApJ, accepted
- Begelman M. C., Sikora M., 1987, ApJ, 322, 650
- Beloborodov A. M., Daigne F., Mochkovitch, R., Uhm Z. L., 2010, arXiv:1003.1265
- Blumenthal G. R., Gould R. J., 1970, Reviews of Modern Physics, vol. 42, issue 2, 237
- Cheng K. S., Zhang J. L., 1996, ApJ, 463, 271
- Cheng K. S., Zhang L., 1998, ApJ, 498, 327
- Chugunov Iu. V., Eidman V. Ia., Suvorov E. V., Astrophysics and Space Science, 1975, 32, L7-L10
- Cocke W. J., Pacholczyk A. G., 1975, ApJ, 195, 279
- Dai Z. G., Lu T., 1998, MNRAS, 298, 87
- Deng X. L., Xia T. S., Liu J., 2005, A&A, 443, 747
- Fermi E., 1949, Physical Review, vol. 75, Issue 8, 1169
- Granot J., Piran T., Sari R., 1999, ApJ, 527, 236
- Gruppen C., Cowan G., Eidelman S., Stroh T. 2005, Astroparticle Physics, Springer, pp. 63-76
- Guetta D., Granot, J. 2003, ApJ, 585, 885
- Harko T., Cheng K. S., 2002, MNRAS, 335, 99
- Hirokani K., Harding A. K., Shibata S., 2003, ApJ, 591, 334
- Jones F. C., 1968, Phys. Rev., 167, 1159
- Kardashev N. S., 1962, Soviet Astronomy, 6, 317
- Lieu R., Axford W. L., 1997, Phys. Rev. E, 55, 1872
- Medvedev M. V., Loeb A. 1999, ApJ, 526, 697
- Medvedev M. V., 2000, ApJ, 540, 704
- Medvedev M. V., Fiore M., Fonseca R. A., Silva L. O., Mori W. B., 2005, ApJ, 618, L75
- Mizuno Y., Pohl M., Niemiec J., Zhang B., Nishikawa K.-I., Hardee P. E., 2010, arXiv:1011.2171
- Piran T. 1999, Phys. Rep., 314, 575
- Press W. H., Teukolsky S. A., Vetterling W. T., Flannery B. P., 1992, Numerical Recipes in Fortran 77, Cambridge University Press, 239-243
- Rossi E. M., Lazzati, D., Salmonson J. D., Ghisellini G., 2004, MNRAS, 354, 86
- Rybicki G. B., Lightman A. P., 1979, Radiative Processes in Astrophysics, John Wiley & Sons, Inc
- Sari R., Piran T., Narayan R., 1998, ApJ, 497, L17
- Sari R., Esin A., 2001, ApJ, 584, 787
- Tavani M. 1996, Phys. Rev. Lett., 76, 3478
- Toma K., Sakamoto T., Zhang B., Hill J. E., McConnell M. L., Bloser P. F., Yamazaki R., Ioka K., Nakamura T., 2009, ApJ, 698, 1042
- Xia T. S., Zhang J. L., 2001, A&A 371, 93
- Yang J. M., Liu J., Zhang, J. L., 2003, Journal of University of Science and Technology of China (in Chinese), 33, 158
- Zhang J. L., Cheng K. S., 1995, Phys. Lett. A, 208, 47
- Zhang J. L., Cheng K. S., 1996, Chin. Astron. Astrophys., 20, 239
- Zhang L., Cheng K. S., 1997, ApJ, 487, 370
- Zhang L., Cheng K. S., 1998, A&A, 335, 234
- Zhang J. L., Yuan Y. F., 1998, ApJ, 493, 826
- Zhang J. L., Xia T. S., Yang J. M., 2000, Phys. Lett. A, 275, 315